Analysis of protein dynamics within the septate junction reveals a highly stable core protein complex that does not include the basolateral polarity protein Discs large

Kenzi Oshima* and Richard G. Fehon‡

Department of Molecular Genetics and Cell Biology, University of Chicago, 920 E. 58th Street, CLSC 925B, Chicago, IL 60637, USA

*Present address: Laboratory of Molecular Bioregulation, Department of Applied Molecular Biosciences, Nagoya University, Furo-cho, Chikusa-ku, Nagoya 464-8601, Japan

‡Author for correspondence (rfehon@uchicago.edu)

Accepted 11 April 2011
Journal of Cell Science 124, 2861-2871
© 2011. Published by The Company of Biologists Ltd
doi:10.1242/jcs.087700

Summary

Barrier junctions prevent pathogen invasion and restrict paracellular leakage across epithelial sheets. To understand how one barrier junction, the septate junction (SJ), is regulated in vivo, we used fluorescence recovery after photobleaching (FRAP) to examine SJ protein dynamics in *Drosophila*. Most SJ-associated proteins, including Coracle, Neurexin IV and Nervana 2, displayed similar, extremely immobile kinetics. Loss of any of these components resulted in dramatically increased mobility of all others, suggesting that they form a single, highly interdependent core complex. Immobilization of SJ core components coincided with formation of the morphological SJ but occurred after their known role in maintaining epithelial polarity, suggesting that these functions are independent. In striking contrast to the core components, the tumor suppressor protein Discs large was much more mobile and its loss did not affect mobility of core SJ proteins, suggesting that it is not a member of this complex, even though it colocalizes with the SJ. Similarly, disruption of endocytosis affected localization of SJ core components, but did not affect their mobility. These results indicate that formation of a stable SJ core complex is separable from its proper subcellular localization, and provide new insights into the complex processes that regulate epithelial polarity and assembly of the SJ.

Key words: Epithelial polarity, Fluorescence recovery after photobleaching, Septate junction

Introduction

Specialized membrane domains, formed by interacting protein networks closely associated with the plasma membrane, are essential to the functions of polarized epithelial cells. One such domain, the apical junctional region, is composed of multiple protein complexes, each consisting of extracellular, transmembrane and membrane-associated cytoplasmic proteins. Regulation of these protein complexes is important both for assembly of intercellular junctions and for their rearrangement during tissue morphogenesis. Biochemical and genetic approaches have identified and characterized many of the individual proteins that constitute intercellular junctions, but have not elucidated the temporal and spatial dynamics of intercellular junctions in living cells. In the case of adherens junctions, recent studies using fluorescently tagged proteins and time-lapse observation analyses have revealed previously unknown dynamics in the regulation of associated protein complexes (Drees et al., 2005; Yamada et al., 2005; Cavey et al., 2008). By contrast, the regulation of the other intercellular junctions, including barrier junctions, is still poorly understood.

Barrier junctions, specifically the vertebrate tight junction (TJ) and the invertebrate septate junction (SJ), have important roles both in restricting paracellular molecular transport across epithelial sheets and in polarizing the plasma membrane and the underlying cortical cytoskeleton along the apical–basal axis (Lamb et al., 1998; Tepass et al., 2001; Furuse and Tsukita, 2006; Cereijido et al., 2008; Miyoshi and Takai, 2008). A hallmark of both TJs and SJs is that they must be stably maintained in both developing and mature epithelia, despite the need for cellular rearrangements that occur in tissues as a result of cell proliferation and migration (Fristrom, 1982; Jinguji and Ishikawa, 1992). For both types of junctions, junctional stability is thought to depend critically on the stability of the underlying protein complexes that form each junction. TJs are formed by two tetra-spanning transmembrane proteins, claudin and occludin, together with cytoplasmic proteins including TJ protein ZO-1 (ZO-1) and TJ protein ZO-2 and Cingulin (Shin et al., 2006; Paris et al., 2008). The claudins in particular have been shown to be key components of TJs and appear to be very stably maintained at the plasma membrane (Furuse et al., 1998; Sasaki et al., 2003; Shen et al., 2008). Similarly, two SJ proteins, Neuroglian (Nrg) and Neurexin IV (Nrx-IV), display limited lateral diffusion in the mature SJ (Laval et al., 2008).

Electron microscopic observation has revealed that the pleated SJs found in ectodermally derived epithelia and glial sheets appear as electron-dense ladder-like structures in the intermembrane space (Tepass and Hartenstein, 1994). SJs are structurally and molecularly homologous to the vertebrate paranodal junction that forms between axons and myelinating glial cells at the edge of the node of Ranvier. This junction distinguishes the node of Ranvier from the internodal regions by segregating ion channels to specific membrane domains (Bhat et al., 2001; Salzer, 2003; Horresh et al., 2010). Previous studies have reported that *Drosophila* SJs consist of at least 12 components, including 10 cell surface and transmembrane proteins. These proteins include three Claudin homologues [Sinuous (Sinu), Megatrachea (Mega) and Kune-kune (Kune)], the Na^+/K^+-ATPase

Journal of Cell Science

α- and β-subunits (ATPα and Nrv2), Nrg, Nrx-IV, Contactin (Cont), Lachesin (Lac), Gliotactin (Gli) and two intracellular components, Coracle (Cora) and Varicose (Vari), that interact with the cytoplasmic tail of transmembrane SJ proteins (Fehon et al., 1994; Baumgartner et al., 1996; Behr et al., 2003; Genova and Fehon, 2003; Paul et al., 2003; Schulte et al., 2003; Faivre-Sarrailh et al., 2004; Llimargas et al., 2004; Wu et al., 2004; Wu et al., 2007; Nelson et al., 2010). Mutations in any of the genes encoding SJ proteins result in disruption of the barrier function and dramatic mislocalization of all other SJ proteins, indicating that they are remarkably interdependent in their functions. In addition, several SJ proteins have been shown to coimmunoprecipitate from tissue extracts, and Cora has been shown to directly interact with the cytoplasmic tail of Nrx-IV, suggesting that they might all function in a single protein complex at the plasma membrane (Ward et al., 1998; Genova and Fehon, 2003; Faivre-Sarrailh et al., 2004).

In addition to their SJ function, Cora, ATPα and Nrx-IV participate in the maintenance of epithelial polarity in the embryonic epidermis. Previous studies have shown that proteins of the Lethal giant larva (Lgl) group, including Lgl, Discs large (Dlg) and Scribbled (Scrib), promote formation of the basolateral membrane domain in the early embryo by antagonizing the action of apical polarity proteins (Bilder and Perrimon, 2000; Bilder et al., 2003; Tanentzapf and Tepass, 2003). Recently, it has been shown that Cora, ATPα, and Nrx-IV, together with the FERM-domain-containing protein Yurt, have a later role in maintaining the basolateral polarity (Laprise et al., 2009). Interestingly, SJ proteins, Yurt and proteins of the Lgl group all colocalize on the lateral membrane, suggesting that they might form a protein complex there (Wu and Beitel, 2004), and Yurt has been shown to coimmunoprecipitate with Nrg (Laprise et al., 2009). However, attempts to demonstrate interactions between SJ proteins and those

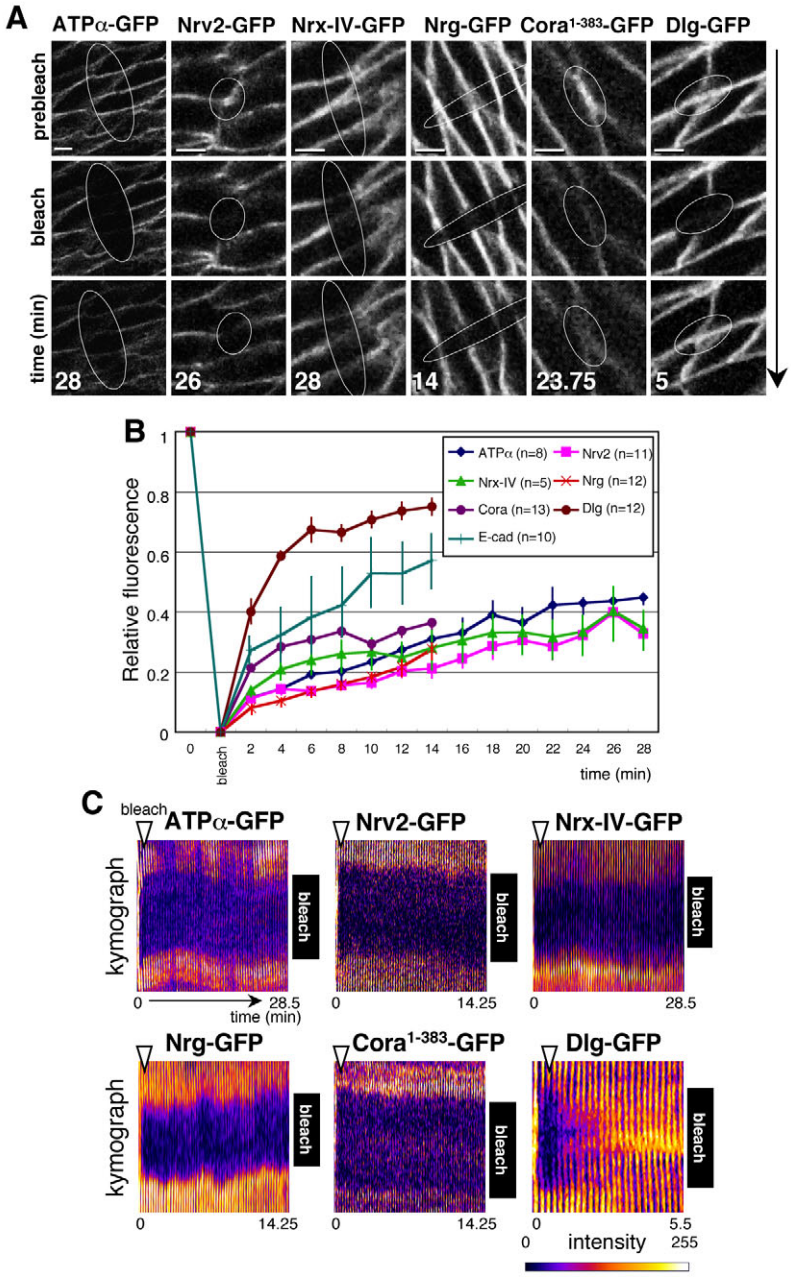

Fig. 1. SJ core proteins display extremely slow FRAP rates. GFP-tagged proteins expressed in the lateral epidermis of stage 14 to 16 embryos were photobleached in the regions indicated (white ellipses). (**A**) Time-series images of photobleached regions for proteins indicated. Note that although Dlg–GFP recovers substantially within 5 minutes, little recovery of SJ core proteins was observed even after much longer time periods. Scale bars: 2 μm. (**B**) Average relative fluorescent recoveries of GFP-tagged SJ proteins. Dlg and E-cadherin, which display faster recoveries, are also plotted. E-cad–GFP was directly driven by ubiquitin promoter. Error bars indicate s.e.m. (**C**) Kymographs showing the recovery over time of a single bleached region of the membrane (taken from supplementary material Movies 1–5, 8–9). White arrowheads indicate time points of photobleaching. Black bars show initial width of the bleached regions. Note the overall lack of recovery for ATPα, Nrv2, Nrx-IV, Nrg, and Cora, as well as the minimal spreading of fluorescence from adjacent, unbleached regions of the membrane. By contrast, Dlg shows rapid recovery and spreading from lateral regions.

Journal of Cell Science

Journal of Cell Science

of the Lgl group have given conflicting results (Ward et al., 1998; Tanentzapf and Tepass, 2003; Schulte et al., 2006).

Although much has been learned about the components of the SJ, the molecular details of how they assemble and maintain such solid structures are largely unclear. To study the dynamics of this barrier junction in vivo, we have used fluorescence recovery after photobleaching (FRAP) to study the behavior of endogenously expressed SJ proteins in living *Drosophila* tissues. Our observations show that SJ core complex formation begins at embryonic stage 13 when cells in the embryonic epidermis individually become competent to form SJs. At least five SJ proteins, including Cora, Nrx-IV, Nrv2, ATPα and Nrg, display similar FRAP kinetics, suggesting that all form a single, stable complex at the plasma membrane. By contrast, the basolateral polarity protein Dlg is much more mobile than these SJ proteins, suggesting that Lgl group proteins are not components of the SJ core protein complex, despite the fact that they localize to the SJ. Surprisingly, FRAP analysis reveals that mutations in *dlg*, *Gliotactin* and genes that affect endocytosis do not affect formation of the SJ core complex, even though they cause dramatic mislocalization of its components. Taken together, these results indicate that formation of the SJ core complex occurs independently of its localization to the SJ, reveal new details regarding the relationship between the SJ and basolateral polarity, and provide insights into the formation and maintenance of barrier junctions.

Results

The septate junction is composed of an extremely immobile multiprotein complex

To understand the mechanism by which SJs are maintained as a stable intercellular barrier, we examined the dynamics of several SJ-associated proteins in vivo. Fly lines expressing four GFP-tagged SJ proteins, ATPα, Nrv2, Nrx-IV and Nrg, were identified from GFP protein trap lines provided by the FlyTrap project (Morin et al., 2001; Buszczak et al., 2007). In these transgenic lines, artificial exons encoding GFP flanked by splice acceptor and splice donor sequences are inserted into an intronic region of each gene. As a result these flies express GFP-tagged proteins under the control of their endogenous promoters. All four lines are homozygous viable, indicating that these GFP-tagged SJ proteins are fully functional and suitable for examining normal protein behavior. GFP-tagged proteins localized at the apico-lateral region in the same manner as the intact proteins and colocalized with an endogenous SJ protein Cora (supplementary material Fig. S1).

To examine the mobility of these proteins in mature SJs, FRAP analysis was performed in the lateral epidermal cells after embryonic stage 14. Even 30 minutes post photobleaching, all four SJ proteins showed less than 50% recovery and had not reached a recovery plateau (Fig. 1A,B and supplementary material Movies 1–4) (Laval et al., 2008). Because embryos at this stage frequently moved and rolled making longer time-lapse observations impossible, it was difficult to determine the mobile fraction and the half recovery time ($t_{1/2}$) of SJ components (see Methods and Materials for details of how these parameters were calculated). Importantly, ATPα, Nrv2, Nrx-IV and Nrg showed similar recovery kinetics (Fig. 1B). Together with the previous reports that SJ proteins coimmunoprecipitate (Genova and Fehon, 2003; Faivre-Sarrailh et al., 2004), these data suggest that these proteins are stably bound in a single complex. By contrast, GFP-tagged *Drosophila* E-cadherin, an adherens junction component, showed a distinct recovery rate from the SJ-associated proteins (Fig. 1B and supplementary material Movie 5). We also checked the mobility of a membrane-targeted GFP in stage 14 embryos. GFP-conjugated CD8 recovered very quickly and its mobile fraction was 81.3±19.6% and $t_{1/2}$ was 3.85±1.11 seconds (n=6). This result shows that these SJ proteins are extremely immobile on the cell membrane compared with other transmembrane proteins.

The limited recovery of SJ fluorescence we observed could either occur by lateral spreading of proteins along the plasma membrane or through membrane trafficking from intracellular compartments. To distinguish these possibilities, we used kymographic analysis to determine whether SJ components diffuse laterally in the plasma membrane (Fig. 1C). Both large area illumination that bleached sections of membrane over a few cells and small area bleaching (about 2 μm diameter) gave similar results. Kymographs clearly displayed the borders between bleached and unbleached regions, which sometimes fluctuated and went out of focus because of dorsal migration of the epidermis at this stage and rotation of the embryo. Bleached regions remained intact during extended observations and did not show spreading from adjacent, non-bleached areas of the plasma membrane, suggesting that SJ proteins are laterally immobile on the membrane (Fig. 1C). To examine this further, we used the fluorescent loss in photobleaching (FLIP) technique in which a small section of the plasma membrane was continuously bleached over time. Continuous photobleaching of ATPα–GFP and Nrx-IV–GFP in a small region of the membrane of wild-type embryonic epidermal cells resulted in only limited fluorescent loss in adjacent regions (Fig. 2A,B and supplementary material Movies 6, 7). These results indicate specific low mobility of these SJ proteins and restricted lateral molecular exchange within the plane of the plasma membrane. Kymographic analysis also showed that fluorescence

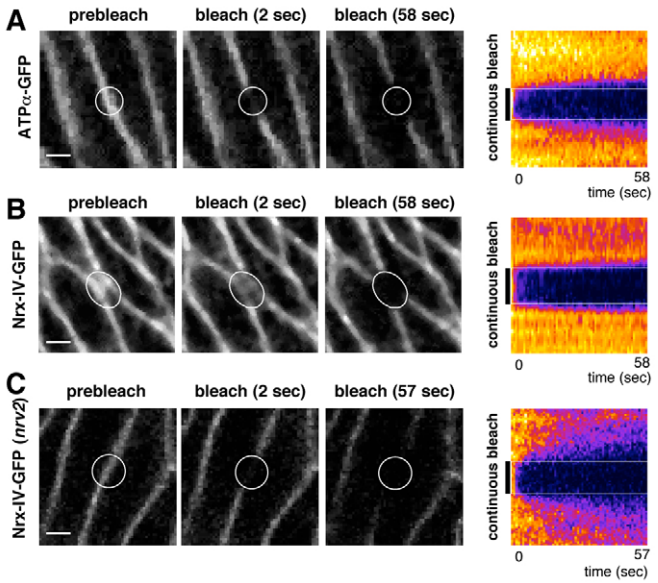

Fig. 2. FLIP analysis of SJ core protein lateral mobility in the membrane. ATPα–GFP (**A**) and Nrx-IV–GFP (**B**) in the wild-type embryonic lateral epidermis, and Nrx-IV–GFP in *nrv2* mutants (**C**) were continuously photobleached. Kymographs (right panels) were generated from the FLIP movies (left panels and supplementary material Movies 6, 7, 12). White lines indicate the bleached areas. The continuously bleached region spreads laterally for Nrx-IV in *nrv2* mutant embryos, but not for ATPα or Nrx-IV in wild-type embryos. Scale bars: 1 μm.

Journal of Cell Science

did not appear to be restored from inside of bleached regions (Fig. 1C), suggesting that SJ protein renewal mediated by the vesicle trafficking is quite slow.

ATPα, Nrv2, Nrx-IV and Nrg are all transmembrane proteins, leading us to wonder whether they might be less mobile than cytoplasmic components of the SJ. Previous studies have identified two cytoplasmic SJ proteins, Cora and Vari, which physically interact with the transmembrane components of the SJ (Ward et al., 1998; Wu et al., 2007). To examine the turnover rate of cytoplasmic SJ components, GFP-tagged FERM domain of Cora ($Cora^{1–383}$), which has been shown to localize to the SJ and to rescue the paracellular barrier defect in *cora*$^{-}$ embryos, was expressed ectopically under control of the heat shock promoter (Ward et al., 2001). $Cora^{1–383}$–GFP showed similar recovery behavior and kinetics to that of the other GFP-tagged membrane SJ proteins (Fig. 1A–C and supplementary material Movie 8). GFP-tagged full-length Cora also gave a similar result (data not shown). These results suggest that the SJ is composed of a highly immobile protein complex containing both transmembrane and cytoplasmic proteins, which we call the SJ core complex.

The Lgl group proteins, Dlg, Scrib and Lgl, function in determining basolateral cell polarity and colocalize with SJ proteins at the apico-lateral region in polarized epithelial cells (Bilder et al., 2000). Thus, some studies have considered them to be components of the SJ (Wu and Beitel, 2004; Schulte et al., 2006). If so, then we would expect these proteins to display similar FRAP mobility to other SJ components. To test this, we observed the mobility of a GFP protein trap line for Dlg, which is also homozygous viable indicating that it is fully functional. Dlg–GFP fluorescence recovered much more quickly than that of any of the SJ proteins we tested (Fig. 1A–C and supplementary material Movie 9). Its mobile fraction was 78.9± 6.2% and $t_{1/2}$ was 1.67±0.46 minutes (n=6). Kymographs showed that Dlg spread laterally along the membrane and was also restored from all over the bleached region, a behavior that is distinctly different from SJ core proteins (Fig. 1C). These differences suggest that Dlg is not a component of the SJ core complex.

Septate junction stability in other epithelia and mitotic cells

To investigate whether SJ stability varies in other tissues or at other stages, we performed FRAP analysis using ATPα, Nrv2, Nrx-IV and Dlg in the larval wing imaginal discs. All displayed similar FRAP kinetics to those we observe in the embryonic epidermis, both in the squamous peripodial cells and in the columnar cells of the wing disc (Fig. 3A,B). Recovery rates in the embryonic hindgut and the larval tracheal cells were also similar (data not shown). These results imply that mature SJs display similar mobility in different epithelial tissues.

The ovarian follicle cells that surround the female germline express multiple SJ-associated proteins but lack morphologically apparent SJs until quite late in oogenesis, after vitellogenesis is

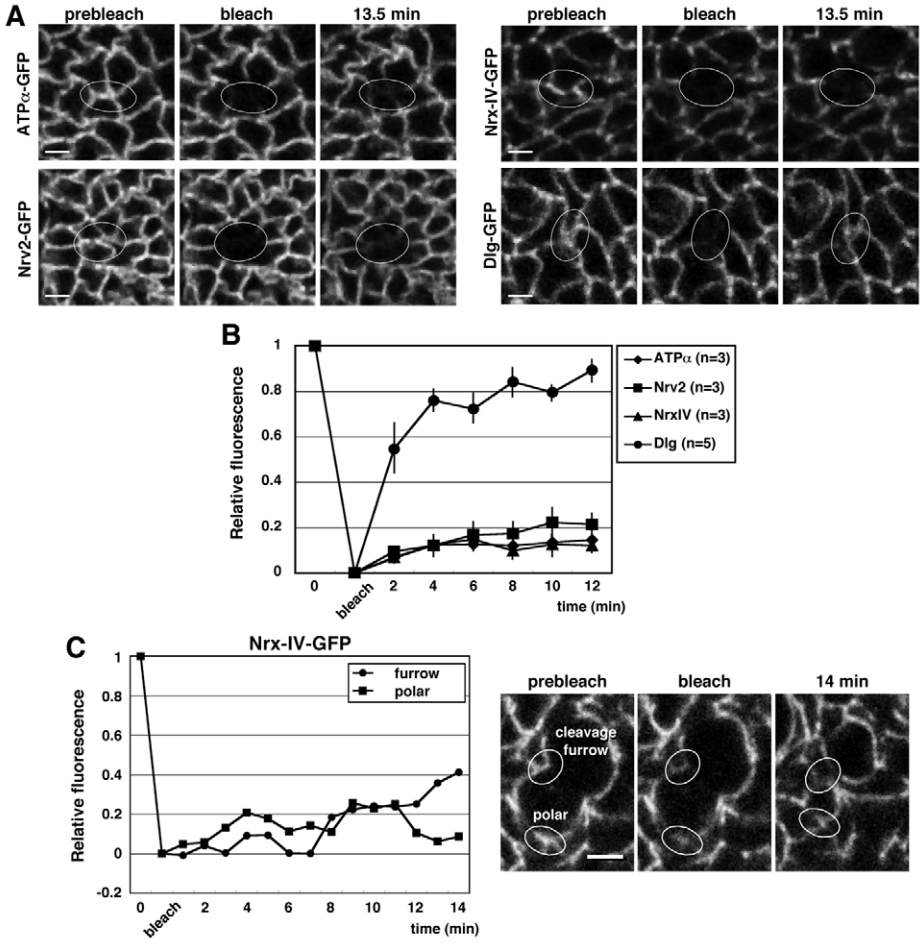

Fig. 3. Mobility of SJ proteins is not altered as cells divide. (**A**) GFP-tagged ATPα, Nrv2, Nrx-IV and Dlg in the columnar cells of wing discs were photobleached. White ellipses indicate bleached regions. (**B**) FRAP of SJ proteins in the columnar cells is plotted. These plots are similar to those for the embryonic epidermis. Error bars indicate s.e.m. (**C**) Nrx-IV–GFP was photobleached in a pair of mitotic columnar cells of the wing disc blade region. Fluorescent recovery in the cleavage furrow and polar region was observed (right panels), and relative fluorescence of this movie was plotted (left graph and supplementary material Movie 10). Scale bars: 1 μm (A), 2 μm (C).

Journal of Cell Science

completed. All follicle cells express Cora, Nrg, ATPα and Dlg along the entire lateral membrane (Woods and Bryant, 1991; Bohrmann and Braun, 1999; Wei et al., 2004), whereas expression of Nrx-IV and Nrv2 was limited just to the polar cells (data not shown). Mobility of Dlg in the follicle cells was comparable to that in other tissues, whereas mobility of ATPα and Nrg was much greater in stage ~4–9 follicle cells compared with that in stage 14 embryonic epidermis (supplementary material Fig. S2), indicating that the immobile complex that forms in other epithelia does not exist in follicle cells at this stage.

Unlike the embryonic epidermis, we frequently observed mitotic cells in the larval wing epithelium. Rapid remodeling of junctional proteins is important for the formation of new junctions between dividing cells, but the mechanism by which cells remodel junctions and simultaneously maintain the barrier function is not clear. Previous studies have shown that dividing cells in vertebrate epithelia maintain epithelial integrity and retain normal tight junction ultrastructure (Pictet et al., 1972; Jinguji and Ishikawa, 1992). To determine whether SJ core complex stability is altered during junctional remodeling, we observed the turnover of SJ proteins in dividing wing disc cells. FRAP analysis of Nrx-IV–GFP and ATPα–GFP in mitotic cells was comparable to that in interphase cells (Fig. 3C; supplementary material Movie 10 and data not shown). Immobile SJ proteins were observed in both the cleavage furrow and peripheral regions of mitotic cells, indicating that cells can rapidly remodel the SJ without disassembling the SJ core complex or requiring significant new synthesis and transport of junctional material to the plasma membrane.

Developmental analysis of SJ assembly

Previous electron microscopic observation has revealed that the ladder-like ultrastructure of the SJ forms between epithelial cells at embryonic stage 14 (Tepass and Hartenstein, 1994), and the paracellular barrier restricting molecular flow forms by stage 15 (Genova and Fehon, 2003; Paul et al., 2003). Although a structural analysis focusing on initial SJ assembly in the insect embryo has been reported (Lane and Swales, 1982), a detailed understanding of how each SJ protein becomes incorporated into developing SJs is still lacking. Previous studies have shown that most SJ proteins, including Mega, Sinu, Gli, Cont, Vari, Lac, Cora and Nrx-IV are expressed before stage 14 (Fehon et al., 1994; Baumgartner et al., 1996; Behr et al., 2003; Schulte et al., 2003; Faivre-Sarrailh et al., 2004; Llimargas et al., 2004; Wu and Beitel, 2004; Wu et al., 2004; Wu et al., 2007), but whether these proteins form a complex at this time is unknown. To explore these matters, we compared the mobility of SJ proteins before and after SJ maturation.

Faint fluorescence of ATPα–GFP, Nrv2–GFP, Nrx-IV–GFP and Nrg–GFP could be discriminated on the cell membrane starting in stage 11 embryos, and their fluorescence continuously increased throughout embryogenesis, concomitant with SJ maturation. Despite the fact that these SJ proteins were expressed as early as stage 11, we found that even at late stage 12, when the germ band was retracting, ATPα–GFP recovered very quickly (Fig. 4A,B and supplementary material Movie 11), similarly to what we observed in stage 4–9 follicle cells. By contrast, after completion of germ band retraction, ATPα was gradually immobilized during early stage 13, and finally this protein became maximally immobile from mid to late stage 13. Nrv2–GFP, Nrx-IV–GFP and Cora$^{1–383}$–GFP also showed a similar stage-dependent immobilization (supplementary material Fig. S3A–C). However, the FRAP kinetics of E-cad–GFP and Dlg–GFP did not change before and after SJ formation (supplementary material Fig. S3D,E). These data clearly show that immobilization at stage 13 is a specific event for SJ core components rather than a common feature of membrane proteins.

To further understand SJ assembly, we examined the localization of GFP-tagged SJ components in the embryonic epidermis from stages 12 to 13. Although expressed before stage 12, ATPα, Nrx-IV and Cora did not display specific localization on the lateral membrane before stage 13 (Fig. 4C and data not shown). These proteins started to accumulate at the apico-lateral region at early stage 13, and at stage 14, displayed the characteristic apico-lateral localization of SJ proteins (Fig. 4C). At stage 13, when SJ

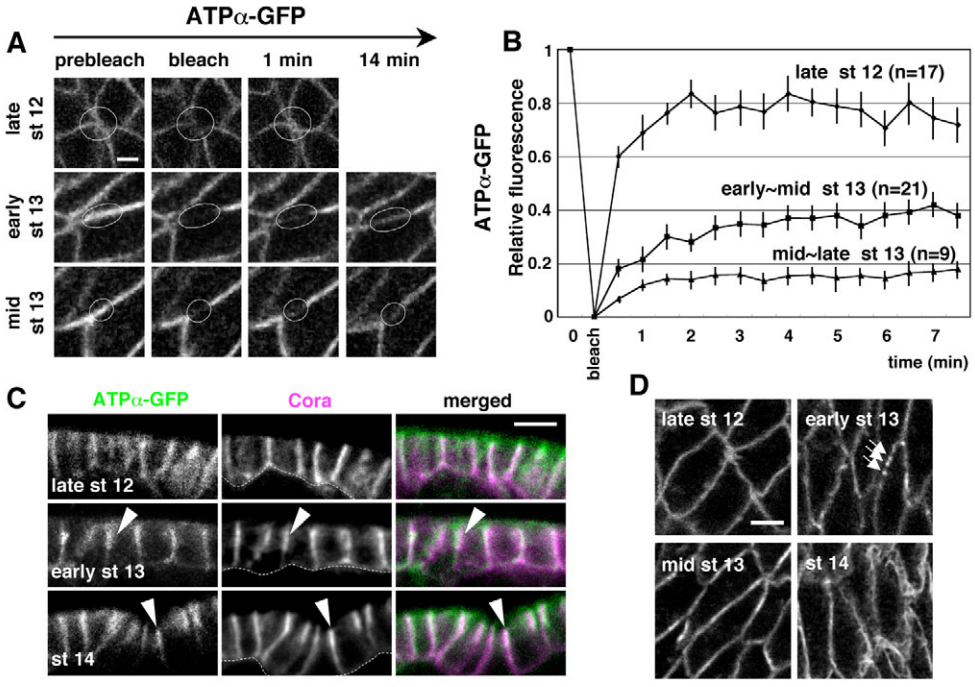

Fig. 4. Immobilization and localization of SJ core proteins occur coordinately during embryonic stage 13. (**A**) ATPα–GFP was photobleached (white ellipses) and then fluorescence recovery was monitored in stage 12 and 13 embryos. (**B**) Average of ATPα–GFP fluorescence recovery at each stage is plotted. Note that the onset of ATPα–GFP immobilization occurred in early stage 13. Error bars indicate s.e.m. (**C**) ATPα–GFP and Cora subcellular localization in stage 12–14 embryos. Vertical views of the lateral epidermis are shown. Arrowheads indicate specific accumulation of the SJ proteins. Dotted lines show the basal side. Note that immobilization and specific localization of ATPα–GFP coincided at stage 13. (**D**) Tangential views of ATPα–GFP in the embryonic lateral epidermis from stage 12 to 14. Starting at early stage 13, regions of locally more intense SJ protein localization are observed along the membrane (arrows). Scale bars: 1 μm (A), 5 μm (C), 2 μm (D).

components begin to localize toward the apico-lateral membrane and show decreased motility, we observed bright spots of ATPα–GFP, Nrv2–GFP and Nrx-IV–GFP in apical focal planes (Fig. 4D and data not shown). FRAP analysis indicated that these bright spots tended to be less mobile than the less-bright regions. During stage 13, these localized spots appeared to progressively coalesce so that they formed continuous mesh-like structures in the later stages (Fig. 4D). Given our FRAP data indicating that SJ core components become immobile on the plasma membrane at the same time, these bright spots might represent assembly of small units of protein complexes which then coalesce to form a continuous SJ band around the cell (Lane and Swales, 1982), similarly to the formation of continuous adherens junctions earlier in development (Tepass and Hartenstein, 1994).

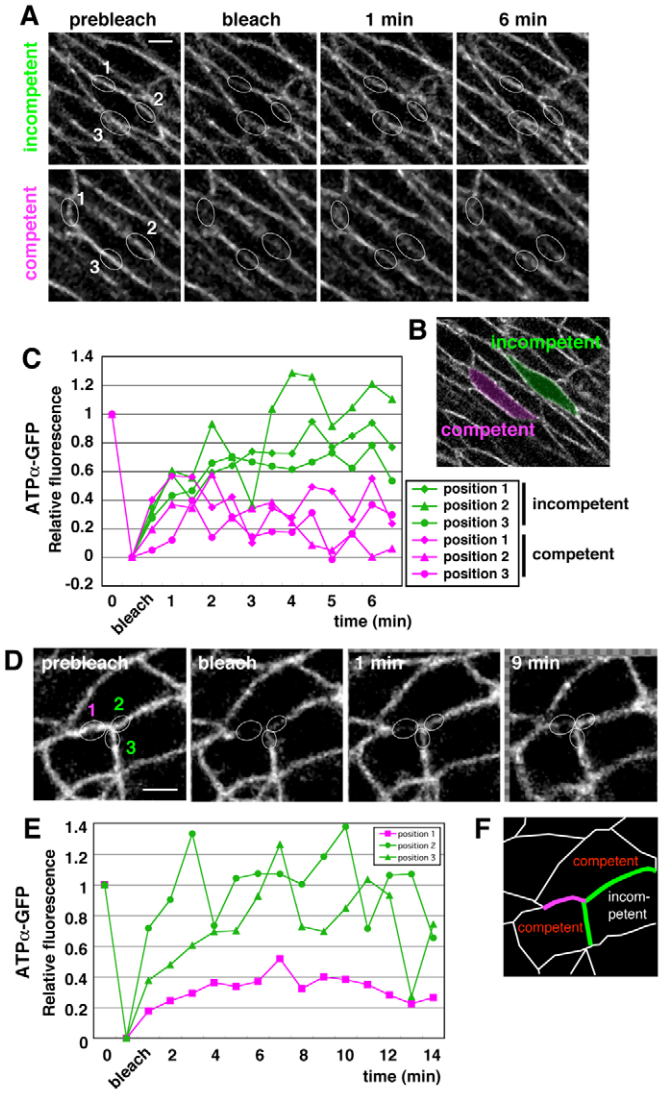

Fig. 5. Epidermal cells in stage 13 embryos individually acquire competency to form immobile SJs. (**A**–**C**) Multiple contacts of two nearby epidermal cells expressing ATPα–GFP were bleached and recovery rates for each contact separately determined. All contacts in the 'competent' cell display less mobility than did those in the 'incompetent' cell. Numbered ellipses in A correspond to the positions plotted in C, which displays fluorescent recovery kinetics. Green and magenta lines display incompetent and competent cells, respectively. (**D**–**F**) A competent epidermal cell can have both mobile and immobile contacts with adjacent cells. (D) Three distinct contacts in epidermal cells expressing ATPα–GFP were photobleached (ellipses marked 1–3). (E) Plots of the fluorescence recovery in regions shown in D. The magenta line indicates the area in which ATPα–GFP was stable, and green lines are the areas in which fluorescence recovered more quickly. (F) An interpretation based on the data in D,E, indicating competent and incompetent cells. Scale bars: 2 μm.

Epidermal cells individually obtain competence to form SJs

Careful comparisons of different epidermal cells in individual stage 13 embryos revealed a further level of complexity in SJ morphogenesis. In single embryos we observed that while some cells at this stage showed stable FRAP dynamics similar to later stage embryos, other, nearby cells displayed dynamics more consistent with early stage 13 embryos (Fig. 5A–C). Because by stage 14 all epidermal cells display SJ protein immobility, this mosaic pattern appears to represent an intermediate phase in which individual cells independently gain 'competence' to form SJs. Interestingly, we occasionally observed individual cells that formed stable junctions with one adjacent cell but not with other contacting cells (Fig. 5D–F), suggesting that an immobile SJ core complex can only form when two competent cells are in contact. A similar phenomenon was observed previously at contacts between wild-type and *cora* mutant cells, where SJs fail to form (Genova and Fehon, 2003). To test this hypothesis, we examined SJ protein mobility at the border between wild-type cells and cells in which Cora expression was suppressed by double-stranded RNA (dsRNA)-mediated knockdown (Fig. 6A). Fluorescence of Nrg–GFP on the border between wild-type and knockdown cells was less bright than between wild-type imaginal disc cells (Fig. 6B,C) and displayed high mobility that was similar to that in the knockdown region (Fig. 6D,E). Based on these observations, we conclude that assembly of an immobile SJ core complex requires contact between two cells that are both competent to assemble the SJ (Fig. 5F).

Genetic analysis of components required for immobile SJ complex formation

Disruption of SJ components, including *mega*, *sinu*, *kune*, *Gli*, *Cont*, *Lac*, *Atpα*, *nrv2*, *Nrx-IV*, *Nrg*, *vari* or *cora*, leads to mislocalization of the other SJ proteins and dysfunction of the paracellular barrier (supplementary material Fig. S4) (Fehon et al., 1994; Baumgartner et al., 1996; Behr et al., 2003; Genova and Fehon, 2003; Paul et al., 2003; Schulte et al., 2003; Faivre-Sarrailh et al., 2004; Llimargas et al., 2004; Wu et al., 2004; Wu et al., 2007; Nelson et al., 2010). In addition, a previous study has shown that mutations in several SJ-associated components affect the FRAP stability of Nrg–GFP and Nrx-IV–GFP (Laval et al., 2008). To further examine the effects of SJ mutations on SJ protein complex formation, we measured the mobility of GFP-tagged ATPα, Nrv2, Nrx-IV and Nrg in different SJ mutant backgrounds (Fig. 7A–D). Fluorescence of all four GFP-tagged proteins recovered much faster in *mega*, *sinu*, *Atpα*, *nrv2*, *Nrx-IV*, *Nrg*, *vari* and *cora* mutant backgrounds than in the controls. To clarify how fluorescence recovered after bleaching, we performed FLIP analysis in a SJ mutant background. Continuous bleaching in the *nrv2* mutant background diminished Nrx-IV–GFP fluorescence, not only in the bleaching point, but also on the neighboring membrane, indicating a significant increase in Nrx-IV lateral mobility in the absence of Nrv2 (Fig. 2D and supplementary material Movie 12). These data

Journal of Cell Science

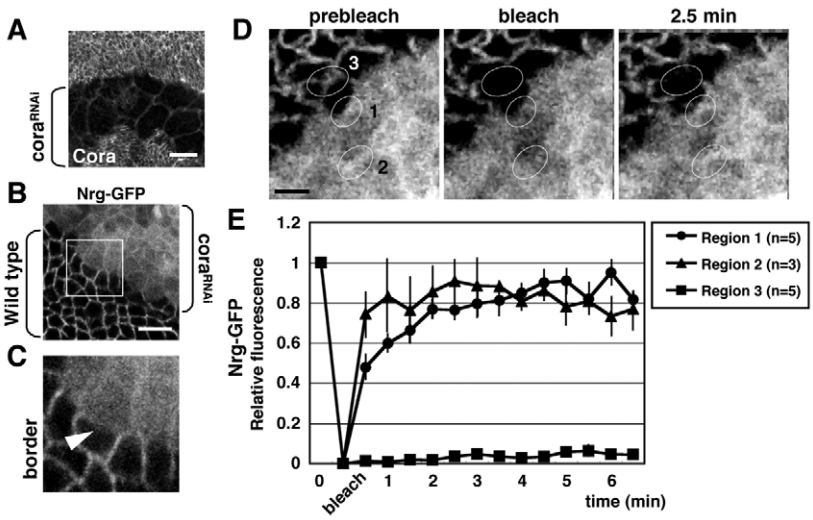

Fig. 6. SJs fail to assemble on the border between *cora*-knockdown and wild-type cells. (**A**) RNAi-mediated knockdown of Cora expression. A portion of a wing imaginal disc expressing double-stranded *cora* RNA under the control of *dpp-Gal4*, stained with anti-Cora antibody. Note that Cora is still expressed in the thin peripodial cell layer that overlaps the *cora*-knockdown region. (**B**,**C**) Nrg–GFP in *cora*-depleted (top right) and wild-type cells (bottom left). Cytoplasmic fluorescence of GFP^{nls} marks the cells expressing double-stranded *cora* RNA, whereas Nrg–GFP is strongly membrane associated. Boxed region is magnified in C. At the border between the intact and *cora*-knockdown cells, membrane-associated Nrg–GFP fluorescence is strongly decreased compared with levels in wild-type cells (arrowhead). (**D**) FRAP of Nrg–GFP in wild-type (region 3) and *cora*-depleted (region 2) cells, and on the border (region 1). (**E**) Average of Nrg–GFP fluorescence recovery in each region is plotted. To avoid measuring cytoplasmic GFP^{nls} fluorescence, only fluorescence at the membrane was imaged. Error bars indicate s.e.m. Scale bars: 20 µm (A), 5 µm (B), 2 µm (D).

suggest that at least Mega, Sinu, ATPα, Nrv2, Nrx-IV, Nrg, Vari and Cora are essential for proper organization of mature, immobile septate junctions.

Previous reports have shown that SJ-associated proteins were not essential for formation and maintenance of the adherens junctions (Genova and Fehon, 2003). Consistent with this, recovery kinetics of E-cadherin did not differ between the control and *cora* mutant backgrounds (data not shown).

Recent studies have shown that several members of the Ly6 protein family in *Drosophila*, including *boudin* (*bou*), *crooked* (*crok*), *coiled* (*cold*) and *crimpled* (*crim*), are essential for SJ formation (Hijazi et al., 2009; Nilton et al., 2010). However, unlike other known SJ components, these Ly6 family proteins do not localize to the SJ, indicating that although they are necessary for SJ morphogenesis, they are not SJ core components. To test their role in SJ core complex formation, we assessed SJ mobility in the Ly6 family mutants. In *bou, crok, cold* and *crim* mutants, SJ core proteins showed similar recovery dynamics as observed in the other SJ mutants, indicating that a stable complex cannot form in the absence of Ly6 family proteins (Fig. 7B–D and data not shown). Because previous studies have suggested that these Ly6 family proteins have a role in intracellular trafficking of SJ components, our results raise the possibility that the SJ core complex is assembled in an intracellular membrane compartment before being trafficked to the lateral plasma membrane.

Gli and endocytic factors regulate SJ localization, but are dispensable for SJ core complex assembly

Although most SJ-associated proteins were essential for organization of an immobile SJ complex, we found one exception in this analysis. This protein was Gliotactin (Gli), which has been shown to be necessary for establishing a functional epithelial barrier and for proper SJ protein localization (supplementary material Fig. S4) (Genova and Fehon, 2003; Schulte et al., 2003). Surprisingly, mobility of SJ core components was unaffected in the Gli^{1} null mutant background and in *Df(2L)BSC255* homozygotes that completely lack the *Gli* gene (Fig. 7A,C,D). Thus, whereas Gli is required for proper localization of the SJ, it is not needed for formation of the stable SJ core complex.

Recent studies have shown that endocytosis is essential for proper SJ formation (Tiklová et al., 2010), but have not distinguished between a role for endocytosis in SJ complex assembly versus proper localization of assembled components. As previously reported, we observed mislocalization of Nrx-IV and elongation of the tracheal dorsal trunk tubes in the *clathrin heavy chain* mutant (chc^{1}) and in the temperature-sensitive *shibire* mutant (shi^{ts}), which encodes the *Drosophila* Dynamin homologue, raised at restrictive temperature (supplementary material Fig. S4 and data not shown). Despite its mislocalization, analysis of Nrx-IV–GFP in both mutant backgrounds revealed FRAP mobilities that were indistinguishable from the wild type (Fig. 7E). This result indicates that although proper subcellular localization of the SJ core complex depends on endocytosis, its formation does not.

Functional interactions between SJ and Lgl group proteins

Although our data indicate that Dlg and SJ proteins have distinct dynamics, Lgl group proteins tightly colocalize with the SJs, suggesting that they are functionally related. To examine this question further, we first compared their localization during SJ formation. Before stage 13, both Dlg and Cora existed uniformly on the lateral membrane (supplementary material Fig. S5). By contrast, by stage 14 these proteins accumulated in the apical half of the lateral membrane and showed strong colocalization.

We next examined the effects of different SJ mutations on Dlg–GFP localization. In *cora*, *Atpα*, *nrv2*, *sinu*, *Gli* and *Nrx-IV* mutants, localization of Dlg–GFP extended further toward the basal area of the lateral membrane when compared with the wild type, although it still accumulated toward the apicolateral region (supplementary material Fig. S4), indicating that Dlg localization is partially dependent on SJ core proteins. However, FRAP studies showed that Dlg dynamics did not change in these mutant backgrounds (Fig. 7F). Interestingly, Dlg–GFP mobility was slightly increased in the *scrib* zygotic mutant background in mid-embryogenesis although its localization was not dramatically affected (Fig. 7F and supplementary material Fig. S4), suggesting that these proteins interact.

Previous studies have examined whether SJs are established in the absence of the basolateral group proteins, with somewhat different results. Specifically, these studies reported that the SJ was formed in the *lgl* mutant but not in the *dlg* mutant (Bilder et al., 2003; Tanentzapf and Tepass, 2003). To further investigate this

Journal of Cell Science

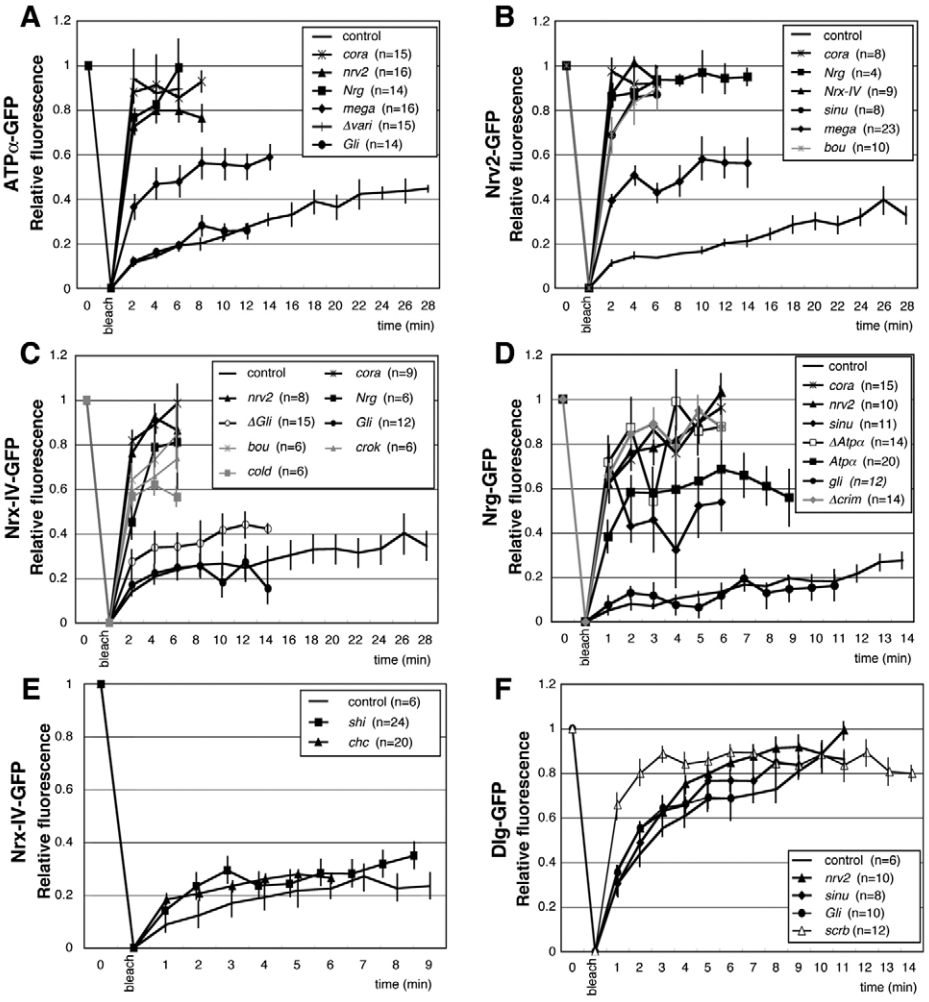

Fig. 7. Loss of SJ components dramatically affects the mobility of SJ core proteins but not Dlg. FRAP of four GFP-tagged SJ proteins (ATPα, Nrv2, Nrx-IV and Nrg) and Dlg in zygotic SJ and endocytic mutant backgrounds in stage 14 or later embryos. Average of the fluorescent recovery of ATPα–GFP (**A**), Nrv2–GFP (**B**), Nrx-IV–GFP (**C**,**E**), Nrg–GFP (**D**) and Dlg–GFP (**F**) is plotted. *Δvari* (A) denotes *Df(2L)Exel7079*, *ΔGli* (C) denotes *Df(2L)BSC255, Δcrim* (D) denotes *Df(3L)ED4470*, and *ΔAtpα* and *Atpα* (D) denote the *Df(3R)ED10811* homozygote and *Df(3R)ED10811/Atpα*^{D1453a} transheterozygote, respectively. Error bars indicate s.e.m.

question, we used FRAP to examine SJ protein stability in the *dlg* maternal/zygotic (MZ) mutant. As described previously, although epidermal cells in the late *dlg* mutant embryos showed polarized localization of an apical marker PATJ (Fig. 8A), Cora and ATPα–GFP mislocalized and did not accumulate along the apicolateral membrane (Fig. 8A,B) (Bilder et al., 2003). However, FRAP analysis revealed that these proteins could display wild-type dynamics in the *dlg* MZ mutant background (Fig. 8D, 'stable'). Specifically, we observed both regions of wild-type dynamics (relatively slow recovery) and much faster recovery (Fig. 8C,D). Stable regions were only apparent in later embryos (stages 16–17), indicating that SJ formation is delayed in the mutants. Taken together, these data indicate a reciprocal interaction between SJ and Lgl group proteins, and suggest that Lgl group proteins facilitate SJ assembly but are not essential for formation of an immobile SJ core complex.

Discussion

Although many proteins have been identified that localize to and are essential for SJ function, the mechanisms by which these proteins assemble into a stable intercellular junction are still poorly understood. Here we have used GFP-tagged SJ proteins to analyze dynamic protein behavior of this barrier junction during morphogenesis. Our results suggest that SJs are composed of a single, highly ordered multiprotein complex, which we call the SJ core complex. Members of the core complex localize to the SJ, and are required for the SJ complex to form and to be stably maintained. Based on these criteria, we propose that the SJ core complex consists of at least eight proteins, including ATPα, Cora, Mega, Nrg, Nrv2, Nrx-IV, Sinu and Vari (Fig. 9). Our results also suggest that members of the Lgl group, which have often been considered to be 'SJ proteins', are not components of the SJ core complex. In support of this idea, FRAP analysis of Dlg–GFP indicates that its mobility at the SJ is much greater than that of the core SJ components we tested. In addition, we found that Dlg–GFP displays normal mobility in the absence of the SJ core complex.

Surprisingly, our studies also reveal that SJ core complex formation and localization to the apical lateral membrane of polarized epithelial cells are two separate processes (Fig. 9). Unlike mutations in core complex components, mutations that affect overall apical–basal polarity (*dlg*) and endocytosis (*shi* and *chc*) do not significantly affect SJ core component mobility in the plasma membrane, even though they have severe effects on its localization. We propose that in these situations, the core complex forms but does not properly coalesce in the apico-lateral region of the membrane where the SJ is normally localized (Fig. 9). Consistent with this idea, Tiklová and colleagues have proposed that endocytosis is required to relocalize SJ-associated proteins from the basolateral to the apico-lateral membrane (Tiklová et al., 2010). Components of the basolateral group, including Scrib, Lgl and

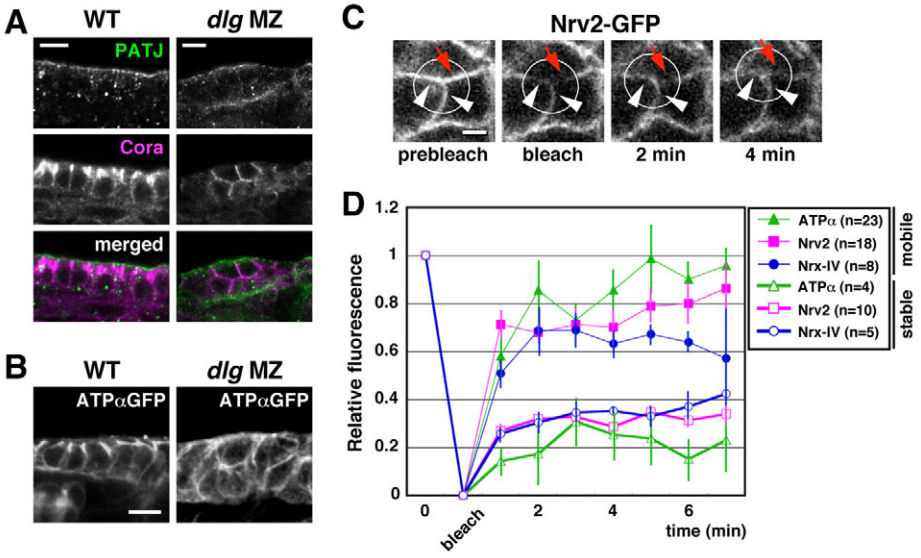

Fig. 8. Immobilization of SJ core proteins occurs independently of Dlg. (**A**,**B**) SJ proteins are mislocalized in the *dlg* maternal/zygotic (MZ) mutant embryos. Cora (A), PATJ (A) and ATPα–GFP (B) are all mislocalized in *dlg* MZ embryos. (**C**) Example of mobile and stable Nrv2–GFP at cell contacts in a stage 17 *dlg* MZ mutant. White arrowheads indicate 'mobile' contacts and the red arrow indicates a 'stable' contact. Areas in which fluorescence recovered to more than 60% within 7 minutes are regarded as 'mobile'. (**D**) Recovery kinetics of ATPα–GFP, Nrv2–GFP and Nrx-IV–GFP in the *dlg* MZ mutant background. Error bars indicate s.e.m. Scale bars: 5 µm (A,B), 2 µm (C).

Dlg, might be required earlier to establish and maintain the membrane domain to which SJ core complexes are relocalized. In the absence of their function, SJs would be expected to either be dispersed along the lateral membrane (as has been observed for *dlg* mutants) (Bilder et al., 2003) or absent.

Loss of Gli, which localizes to the tricellular junction, but not along the lateral membrane between two cells, also affects SJ core component localization but not mobility. Padash-Barmchi and co-workers have reported that phosphorylation of conserved tyrosines in the cytoplasmic tail of Gli triggers its internalization through an endocytic process (Padash-Barmchi et al., 2010). How endocytosis of Gli has a role in SJ localization remains unclear, but the observation that both *Gli* and endocytosis mutants affect SJ protein localization but not formation of the SJ core complex suggests that Gli might regulate endocytosis of formed SJ core complexes from the plasma membrane.

The low mobility of the SJ core proteins we describe resembles that observed for mammalian Claudin proteins in the TJ (Sasaki et al., 2003; Shen et al., 2008), perhaps suggesting that a similar core complex also forms in the TJ. However, two other proteins known to be essential for TJ function, ZO-1 and Occludin, exhibit distinctly faster mobilities (Shen et al., 2008). This observation, together with the fact that Claudin-1 exogenously expressed in fibroblasts forms immobile strands in the plasma membrane (Sasaki et al., 2003), suggests that although Claudin-1 forms a highly stable complex with itself, other TJ components are not as stably associated. This situation clearly differs from the SJ, where removal of even one core component results in severely increased mobility and disrupted subcellular localization of all other components.

The observed immobility of SJ proteins at the plasma membrane seems consistent with freeze-fracture studies showing that the SJ is composed of an almost crystalline array of protein particles in the lateral plasma membrane (Noirot et al., 1979), and with the need for epithelia, such as those that line the gut, to form and maintain a tight seal that blocks diffusion across the epithelial layer (Lamb et al., 1998; Furuse and Tsukita, 2006). At the same time, however, it is clear that cells in developing, proliferating epithelia must be able to change cell-to-cell contacts and therefore rearrange junctional complexes. Remarkably, once SJs became established in late stage 13 embryos, we found no evidence of altered mobility of SJ core components in cells actively rearranging contacts, for example, in the imaginal epithelium as cells divide. How cells regulate assembly and disassembly of SJs remains unclear, although the fact that we did not observe changes in SJ mobility suggests that in mature epithelia the core components might assemble into intracellular complexes that are then slowly trafficked to the SJ. Recent studies of several Ly6 family proteins, which are essential for SJ formation and maintenance but do not themselves appear to localize to the SJ, indicate that they might participate in assembly of the SJ core complex in an intracellular compartment (Hijazi et al., 2009; Nilton et al., 2010). Consistent with this model, we found that loss of any one of the four Ly6 proteins tested resulted in increased SJ core protein mobility.

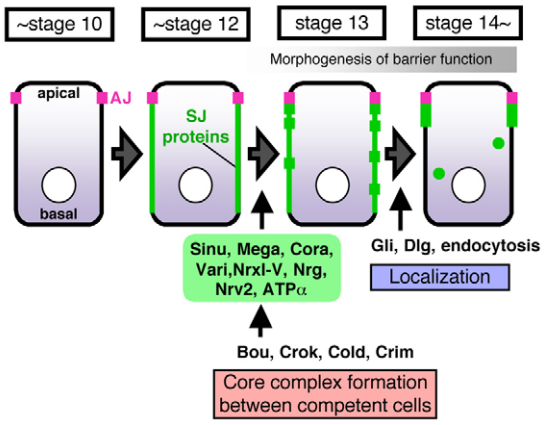

Fig. 9. Schematic model of SJ maturation during embryogenesis. SJ proteins are initially highly mobile on the lateral membrane (stage 12), but in stage 13, Sinu, Mega, Cora, Vari, Nrx-IV, Nrg, Nrv2 and ATPα begin to form a stable SJ core complex just basal to the AJ. Four Ly6-like proteins (Bou, Crok, Cold and Crim) are necessary for this process. In addition, proper localization of the core complex requires Dlg, Gli and endocytosis. See Discussion for further details.'

Journal of Cell Science

Previous work indicated that wild-type cells cannot assemble a SJ on the border with a *cora* mutant cell, suggesting that stable SJ core complex assembly requires both intracellular and intercellular protein interactions (Genova and Fehon, 2003). In the course of our studies, we observed a similar situation among different cells in the epidermis of wild-type stage 13 embryos. At this stage, we found that the epidermis appears to be a mosaic of cells that are competent to form SJs together with those that have not yet gained this competence. Consistent with this idea, we observed individual cells that displayed highly immobile SJ proteins along contacts with one cell, but not in the contact region with another cell (Fig. 5D–F). These observations suggest that epidermal cells individually gain the ability to form SJs, and support the notion that formation of a stable SJ requires cooperative interactions between adjacent cells.

An interesting question raised in these studies is whether SJ proteins have functions before their assembly into immobile complexes at stage 13. As noted previously, many SJ proteins are expressed as early as stage 10. One possible early function is suggested by a recent study implicating Cora, Nrx-IV and ATPα as components of an epithelial polarity mechanism together with Yurt, a FERM-domain-containing protein that also localizes in the region of the SJ (Laprise et al., 2009). This Yurt-dependent polarity mechanism appears to be partially redundant with Lgl group proteins and functions in stage 11–13 embryos, before SJ core proteins display decreased mobility. In addition, several SJ proteins are expressed in follicle cells throughout egg chamber development, even though SJs are not morphologically apparent until stage 10 of oogenesis (Mahowald, 1972). In the follicle cells, Nrg has been suggested to stabilize epithelial polarity and maintain epithelial integrity together with Dlg (Wei et al., 2004). These observations suggest that formation of an immobile complex is not required for the role of Cora, Nrx-IV, Nrg and ATPα in epithelial polarity, and therefore that their function in polarity might be quite distinct from their function in SJ morphogenesis.

The results presented here demonstrate that the SJ core complex assembles rapidly in the stage 13 embryo, and that once established, is very stably maintained in epithelial cells throughout development. The use of ‘gene trap’ lines that label endogenously expressed, fully functional SJ proteins with GFP tags has provided a powerful tool for examining the dynamics of this barrier junction in living tissues. However, the nature of the cue that conveys competence to form the core complex remains unclear. Likely possible mechanisms for triggering assembly might include: (1) accumulation of a crucial concentration of one or more necessary components; (2) post-translational modification of components; or (3) temporally regulated expression of an as yet unidentified SJ protein. Further work will be required to understand the complicated interplay between cell–cell signaling and intracellular cues that regulates SJ core complex assembly in developing epithelia.

Materials and Methods

Drosophila genetics

All flies were kept at 25 or 22°C. GFP protein trap lines used in this study were ATPα–GFP (ZCL1792), Nrv2–GFP (ZCL2903), Nrx-IV–GFP (CA06597), Nrg–GFP (G305) and Dlg–GFP (CC01936), provided by the FlyTrap Project. Genotypes used to examine GFP-tagged proteins in SJ mutant backgrounds are listed in supplementary material Table S1.

E-cadherin–GFP was directly driven by the ubiquitin promoter. *UAS-E-cadherin-GFP* (Oda and Tsukita, 1999) and *UAS-mCD8-GFP* (Lee and Luo, 1999) were driven by the *en^{ciBe}-Gal4* driver in wild-type embryos and by *ubiquitin-Gal4* in *cora* mutants. Cora$^{1–383}$–GFP fused to the heat shock promoter (Ward et al., 1998) was induced by incubating at 38°C for 45 minutes twice, separated by 30 minutes, at 25°C. The UAS-cora-RNAi lines, 9787 and 9788, were obtained from the Vienna Drosophila RNAi Center (VDRC; Vienna, Austria). To deplete Cora expression by RNAi in wing discs, *Nrg-GFP; UAS-cora-RNAi* was crossed to *dpp^{blink}-gal4, UAS-GFP^{nls}* flies. *shi^{ts}* mutants were collected at 22°C for 10 hrs and then shifted to 35°C for 4.5 hrs. Germline clones to remove both maternal and zygotic gene products (MZ mutants) of *dlg^{14}* were produced using the *ovo^{D}* technique as previously described (Bilder et al., 2003) and crossing with (1) *FM7a, dfd-GMR-YFP/Y;* (2) *nrv2-GFP, FM7a, dfd-GMR-YFP/Y; Atpα-GFP,* or (3) *FM7a dfd-GMR-YFP/Y; Nrx-IV-GFP* lines.

Live imaging and image analysis

Embryos were aged at 22°C or 25°C and staged as previously described (Campos-Ortega and Hartenstein, 1997). Embryos dechorionated in 50% bleach were rinsed, mounted on coverslips coated with heptane glue, and covered with halocarbon oil 700 (Sigma). The coverslips were then set on a window chamber (Kiehart et al., 1994). Observation and photobleaching were performed with a laser-scanning confocal microscope (LSM510) using the LSM acquisition software (Carl Zeiss) and a 40× NA 1.3 EC Plan-NeoFluar objective. GFP was photobleached with 100% output of 488 nm laser for 25.56 μseconds/pixel twice for FRAP analysis and continuously for FLIP. Except when multiple cells were treated, the region photobleached was kept between 2 to 5 μm in diameter to ensure consistent results. Wing discs from wandering 3rd-instar larvae and ovaries from female adults were dissected, placed on a microscope slide in Schneider’s *Drosophila* medium (Invitrogen) containing 10% Insect Medium Supplement (Sigma), and covered with a coverslip using double-sided tape as a spacer. To reduce evaporation, edges of coverslips were sealed with halocarbon oil 700.

Captured images were despeckled once with a 0.5 pixel median filter and fluorescence recovery was analyzed by measuring the mean gray value along the plasma membrane of bleached areas with ImageJ (National Institutes of Health). For FRAP data analysis, non-specific background photobleaching at each time point was controlled for by measuring fluorescence loss in separate unbleached plasma membrane regions and calculating recovery relative to this value. Lateral shifting in the time-lapse video images due to embryo movement was corrected using iSEMS (Kato and Hayashi, 2008). Kymographs were generated using Adobe Photoshop CS4 (Adobe) and ImageJ. The mobile fraction was calculated as the full recovery value once recovery had reached a plateau (Reits and Neefjes, 2001). $t_{1/2}$ was calculated as the time required for recovery of bleached fluorescence to half of its maximum recovery value (Yguerabide et al., 1982).

Immunohistochemistry

Dechorionated embryos were fixed in 4% paraformaldehyde:heptane (1:1) for 45 minutes with vigorous shaking at 300 r.p.m. Wing discs isolated from wandering 3rd-instar larvae were fixed and stained as previously described (Fehon et al., 1991). Primary antibodies were used at the following conditions: guinea pig anti-Cora, 1:10,000; rabbit anti-GFP (Molecular Probes), 1:1000; rabbit anti-PATJ (provided by M. Bhat, University of North Carolina, Chapel Hill, NC), 1:10,000; mouse monoclonal anti-Dlg (4F3) (Developmental Studies Hybridoma Bank), 1:500. Confocal images were taken on a laser-scanning confocal microscope (LSM510) using either a 40× NA 1.3 EC Plan-NeoFluar objective or a 20× NA 0.8 Plan-Apochromat objective. Colors and sizes of the acquired were then modified Adobe Photoshop CS4.

We thank A. E. Uv, D. Bilder, J. Zallen, S. Hayashi, the FlyTrap Project, the Vienna Drosophila RNAi Center, and the Bloomington Stock Center for providing fly stocks; M. Bhat and the Developmental Studies Hybridoma Bank for providing antibodies; K. Kato providing for iSEMS software; A. E. Uv, G. J. Beitel, I. Rebay, and J. R. Turner for comments on the manuscript; members of the Fehon and Rebay laboratories for suggestions throughout this work. This work was funded by grant GM074063 from the National Institutes of Health. Deposited in PMC for release after 12 months.

Supplementary material available online at
http://jcs.biologists.org/cgi/content/full/124/16/2861/DC1

References

Baumgartner, S., Littleton, J. T., Broadie, K., Bhat, M. A., Harbecke, R., Lengyel, J. A., Chiquet-Ehrismann, R., Prokop, A. and Bellen, H. J. (1996). A Drosophila neurexin is required for septate junction and blood-nerve barrier formation and function. *Cell* **87**, 1059-1068.

Behr, M., Riedel, D. and Schuh, R. (2003). The claudin-like megatrachea is essential in septate junctions for the epithelial barrier function in Drosophila. *Dev. Cell* **5**, 611-620.

Bhat, M. A., Rios, J. C., Lu, Y., Garcia-Fresco, G. P., Ching, W., St Martin, M., Li, J., Einheber, S., Chesler, M., Rosenbluth, J. et al. (2001). Axon-glia interactions and the domain organization of myelinated axons requires neurexin IV/Caspr/Paranodin. *Neuron* **30**, 369-383.

Bilder, D. and Perrimon, N. (2000). Localization of apical epithelial determinants by the basolateral PDZ protein Scribble. *Nature* **403**, 676-680.

Bilder, D., Li, M. and Perrimon, N. (2000). Cooperative regulation of cell polarity and growth by Drosophila tumor suppressors. *Science* **289**, 113-116.
Bilder, D., Schober, M. and Perrimon, N. (2003). Integrated activity of PDZ protein complexes regulates epithelial polarity. *Nat. Cell Biol.* **5**, 53-58.
Bohrmann, J. and Braun, B. (1999). Na,K-ATPase and V-ATPase in ovarian follicles of Drosophila melanogaster. *Biol. Cell* **91**, 85-98.
Buszczak, M., Paterno, S., Lighthouse, D., Bachman, J., Planck, J., Owen, S., Skora, A. D., Nystul, T. G., Ohlstein, B., Allen, A. et al. (2007). The carnegie protein trap library: a versatile tool for Drosophila developmental studies. *Genetics* **175**, 1505-1531.
Campos-Ortega, J. A. and Hartenstein, V. (1997). *The Embryonic Development of Drosophila melanogaster*. Berlin, New York: Springer.
Cavey, M., Rauzi, M., Lenne, P. F. and Lecuit, T. (2008). A two-tiered mechanism for stabilization and immobilization of E-cadherin. *Nature* **453**, 751-756.
Cereijido, M., Contreras, R. G., Shoshani, L., Flores-Benitez, D. and Larre, I. (2008). Tight junction and polarity interaction in the transporting epithelial phenotype. *Biochim. Biophys. Acta* **1778**, 770-793.
Drees, F., Pokutta, S., Yamada, S., Nelson, W. J. and Weis, W. I. (2005). Alpha-catenin is a molecular switch that binds E-cadherin-beta-catenin and regulates actin-filament assembly. *Cell* **123**, 903-915.
Faivre-Sarrailh, C., Banerjee, S., Li, J., Hortsch, M., Laval, M. and Bhat, M. A. (2004). Drosophila contactin, a homolog of vertebrate contactin, is required for septate junction organization and paracellular barrier function. *Development* **131**, 4931-4942.
Fehon, R. G., Johansen, K., Rebay, I. and Artavanis-Tsakonas, S. (1991). Complex cellular and subcellular regulation of notch expression during embryonic and imaginal development of Drosophila: implications for notch function. *J. Cell Biol.* **113**, 657-669.
Fehon, R. G., Dawson, I. A. and Artavanis-Tsakonas, S. (1994). A Drosophila homologue of membrane-skeleton protein 4.1 is associated with septate junctions and is encoded by the coracle gene. *Development* **120**, 545-557.
Fristrom, D. K. (1982). Septate junctions in imaginal disks of Drosophila: a model for the redistribution of septa during cell rearrangement. *J. Cell Biol.* **94**, 77-87.
Furuse, M. and Tsukita, S. (2006). Claudins in occluding junctions of humans and flies. *Trends Cell Biol.* **16**, 181-188.
Furuse, M., Fujita, K., Hiiragi, T., Fujimoto, K. and Tsukita, S. (1998). Claudin-1 and -2: novel integral membrane proteins localizing at tight junctions with no sequence similarity to occludin. *J. Cell Biol.* **141**, 1539-1550.
Genova, J. L. and Fehon, R. G. (2003). Neuroglian, Gliotactin, and the Na+/K+ ATPase are essential for septate junction function in Drosophila. *J. Cell Biol.* **161**, 979-989.
Hijazi, A., Masson, W., Augé, B., Waltzer, L., Haenlin, M. and Roch, F. (2009). boudin is required for septate junction organisation in Drosophila and codes for a diffusible protein of the Ly6 superfamily. *Development* **136**, 2199-2209.
Horresh, I., Bar, V., Kissil, J. L. and Peles, E. (2010). Organization of myelinated axons by Caspr and Caspr2 requires the cytoskeletal adapter protein 4.1B. *J. Neurosci.* **30**, 2480-2489.
Jinguji, Y. and Ishikawa, H. (1992). Electron microscopic observations on the maintenance of the tight junction during cell division in the epithelium of the mouse small intestine. *Cell Struct. Funct.* **17**, 27-37.
Kato, K. and Hayashi, S. (2008). Practical guide of live imaging for developmental biologists. *Dev. Growth Differ.* **50**, 381-390.
Kiehart, D. P., Montague, R. A., Rickoll, W. L., Foard, D. and Thomas, G. H. (1994). High-resolution microscopic methods for the analysis of cellular movements in Drosophila embryos. *Methods Cell Biol.* **44**, 507-532.
Lamb, R. S., Ward, R. E., Schweizer, L. and Fehon, R. G. (1998). Drosophila coracle, a member of the protein 4.1 superfamily, has essential structural functions in the septate junctions and developmental functions in embryonic and adult epithelial cells. *Mol. Biol. Cell* **9**, 3505-3519.
Lane, N. J. and Swales, L. S. (1982). Stages in the assembly of pleated and smooth septate junctions in developing insect embryos. *J. Cell Sci.* **56**, 245-262.
Laprise, P., Lau, K. M., Harris, K. P., Silva-Gagliardi, N. F., Paul, S. M., Beronja, S., Beitel, G. J., McGlade, C. J. and Tepass, U. (2009). Yurt, Coracle, Neurexin IV and the Na(+),K(+)-ATPase form a novel group of epithelial polarity proteins. *Nature* **459**, 1141-1145.
Laval, M., Bel, C. and Faivre-Sarrailh, C. (2008). The lateral mobility of cell adhesion molecules is highly restricted at septate junctions in Drosophila. *BMC Cell Biol.* **9**, 38.
Lee, T. and Luo, L. (1999). Mosaic analysis with a repressible cell marker for studies of gene function in neuronal morphogenesis. *Neuron* **22**, 451-461.
Llimargas, M., Strigini, M., Katidou, M., Karagogeos, D. and Casanova, J. (2004). Lachesin is a component of a septate junction-based mechanism that controls tube size and epithelial integrity in the Drosophila tracheal system. *Development* **131**, 181-190.
Mahowald, A. P. (1972). Ultrastructural observations on oogenesis in Drosophila. *J. Morphol.* **137**, 29-48.
Miyoshi, J. and Takai, Y. (2008). Structural and functional associations of apical junctions with cytoskeleton. *Biochim. Biophys. Acta* **1778**, 670-691.
Morin, X., Daneman, R., Zavortink, M. and Chia, W. (2001). A protein trap strategy to detect GFP-tagged proteins expressed from their endogenous loci in Drosophila. *Proc. Natl. Acad. Sci. USA* **98**, 15050-15055.
Nelson, K. S., Furuse, M. and Beitel, G. J. (2010). The Drosophila claudin kune-kune is required for septate junction organization and tracheal tube size control. *Genetics* **185**, 831-839.
Nilton, A., Oshima, K., Zare, F., Byri, S., Nannmark, U., Nyberg, K. G., Fehon, R. G. and Uv, A. E. (2010). Crooked, Coiled and Crimpled are three Ly6-like proteins required for proper localization of septate junction components. *Development* **137**, 2427-2437.
Noirot, C., Smith, D. S., Cayer, M. L. and Noirot-Timothée, C. (1979). The organization and isolating function of insect rectal sheath cells: a freeze-fracture study. *Tissue Cell* **11**, 325-336.
Oda, H. and Tsukita, S. (1999). Nonchordate classic cadherins have a structurally and functionally unique domain that is absent from chordate classic cadherins. *Dev. Biol.* **216**, 406-422.
Padash-Barmchi, M., Browne, K., Sturgeon, K., Jusiak, B. and Auld, V. J. (2010). Control of Gliotactin localization and levels by tyrosine phosphorylation and endocytosis is necessary for survival of polarized epithelia. *J. Cell Sci.* **123**, 4052-4062.
Paris, L., Tonutti, L., Vannini, C. and Bazzoni, G. (2008). Structural organization of the tight junctions. *Biochim. Biophys. Acta* **1778**, 646-659.
Paul, S. M., Ternet, M., Salvaterra, P. M. and Beitel, G. J. (2003). The Na+/K+ ATPase is required for septate junction function and epithelial tube-size control in the Drosophila tracheal system. *Development* **130**, 4963-4974.
Pictet, R. L., Clark, W. R., Williams, R. H. and Rutter, W. J. (1972). An ultrastructural analysis of the developing embryonic pancreas. *Dev. Biol.* **29**, 436-467.
Reits, E. A. and Neefjes, J. J. (2001). From fixed to FRAP: measuring protein mobility and activity in living cells. *Nat. Cell Biol.* **3**, E145-E147.
Salzer, J. L. (2003). Polarized domains of myelinated axons. *Neuron* **40**, 297-318.
Sasaki, H., Matsui, C., Furuse, K., Mimori-Kiyosue, Y., Furuse, M. and Tsukita, S. (2003). Dynamic behavior of paired claudin strands within apposing plasma membranes. *Proc. Natl. Acad. Sci. USA* **100**, 3971-3976.
Schulte, J., Tepass, U. and Auld, V. J. (2003). Gliotactin, a novel marker of tricellular junctions, is necessary for septate junction development in Drosophila. *J. Cell Biol.* **161**, 991-1000.
Schulte, J., Charish, K., Que, J., Ravn, S., MacKinnon, C. and Auld, V. J. (2006). Gliotactin and Discs large form a protein complex at the tricellular junction of polarized epithelial cells in Drosophila. *J. Cell Sci.* **119**, 4391-4401.
Shen, L., Weber, C. R. and Turner, J. R. (2008). The tight junction protein complex undergoes rapid and continuous molecular remodeling at steady state. *J. Cell Biol.* **181**, 683-695.
Shin, K., Fogg, V. C. and Margolis, B. (2006). Tight junctions and cell polarity. *Annu. Rev. Cell Dev. Biol.* **22**, 207-235.
Tanentzapf, G. and Tepass, U. (2003). Interactions between the crumbs, lethal giant larvae and bazooka pathways in epithelial polarization. *Nat. Cell Biol.* **5**, 46-52.
Tepass, U. and Hartenstein, V. (1994). The development of cellular junctions in the Drosophila embryo. *Dev. Biol.* **161**, 563-596.
Tepass, U., Tanentzapf, G., Ward, R. and Fehon, R. (2001). Epithelial cell polarity and cell junctions in Drosophila. *Annu. Rev. Genet.* **35**, 747-784.
Tiklová, K., Senti, K.-A., Wang, S., Gräslund, A. and Samakovlis, C. (2010). Epithelial septate junction assembly relies on melanotransferrin iron binding and endocytosis in Drosophila. *Nat. Cell Biol.* **12**, 1071-1078.
Ward, R. E., Lamb, R. S. and Fehon, R. G. (1998). A conserved functional domain of Drosophila coracle is required for localization at the septate junction and has membrane-organizing activity. *J. Cell Biol.* **140**, 1463-1473.
Ward, R. E., Schweizer, L., Lamb, R. S. and Fehon, R. G. (2001). The protein 4.1, ezrin, radixin, moesin (FERM) domain of Drosophila Coracle, a cytoplasmic component of the septate junction, provides functions essential for embryonic development and imaginal cell proliferation. *Genetics* **159**, 219-228.
Wei, J., Hortsch, M. and Goode, S. (2004). Neuroglian stabilizes epithelial structure during Drosophila oogenesis. *Dev. Dyn.* **230**, 800-808.
Woods, D. F. and Bryant, P. J. (1991). The discs-large tumor suppressor gene of Drosophila encodes a guanylate kinase homolog localized at septate junctions. *Cell* **66**, 451-464.
Wu, V. M. and Beitel, G. J. (2004). A junctional problem of apical proportions: epithelial tube-size control by septate junctions in the Drosophila tracheal system. *Curr. Opin. Cell Biol.* **16**, 493-499.
Wu, V. M., Schulte, J., Hirschi, A., Tepass, U. and Beitel, G. J. (2004). Sinuous is a Drosophila claudin required for septate junction organization and epithelial tube size control. *J. Cell Biol.* **164**, 313-323.
Wu, V. M., Yu, M. H., Paik, R., Banerjee, S., Liang, Z., Paul, S. M., Bhat, M. A. and Beitel, G. J. (2007). Drosophila Varicose, a member of a new subgroup of basolateral MAGUKs, is required for septate junctions and tracheal morphogenesis. *Development* **134**, 999-1009.
Yamada, S., Pokutta, S., Drees, F., Weis, W. I. and Nelson, W. J. (2005). Deconstructing the cadherin-catenin-actin complex. *Cell* **123**, 889-901.
Yguerabide, J., Schmidt, J. A. and Yguerabide, E. E. (1982). Lateral mobility in membranes as detected by fluorescence recovery after photobleaching. *Biophys. J.* **40**, 69-75.

Journal of Cell Science

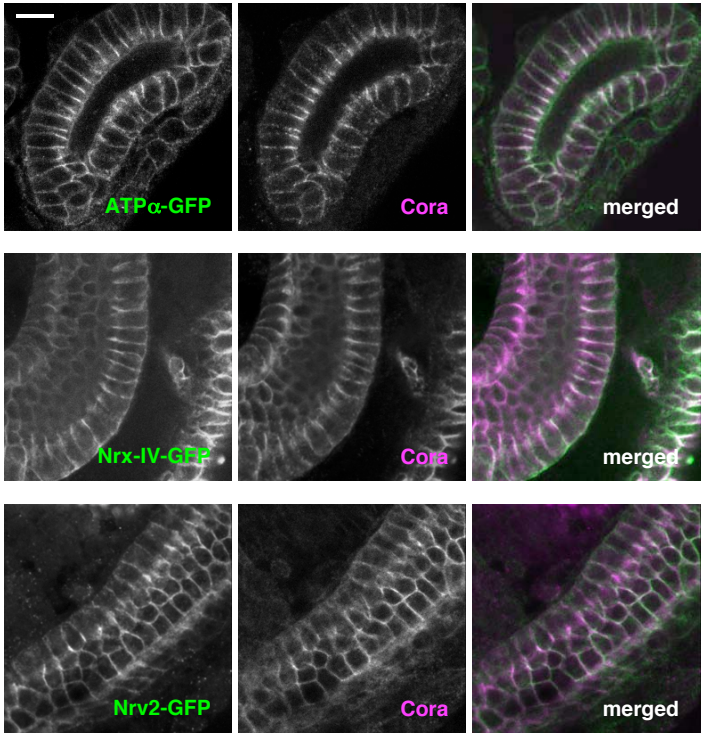
ATPα-GFP
Cora
merged
Nrx-IV-GFP
Cora
merged
Nrv2-GFP
Cora
merged

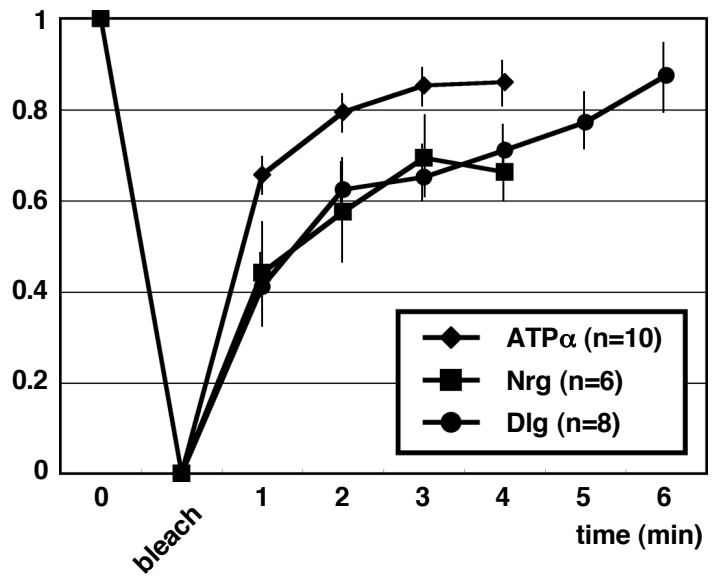
1
0.8
0.6
0.4
0.2
0
0
bleach
1
2
3
4
5
6
time (min)
ATPα (n=10)
Nrg (n=6)
Dlg (n=8)

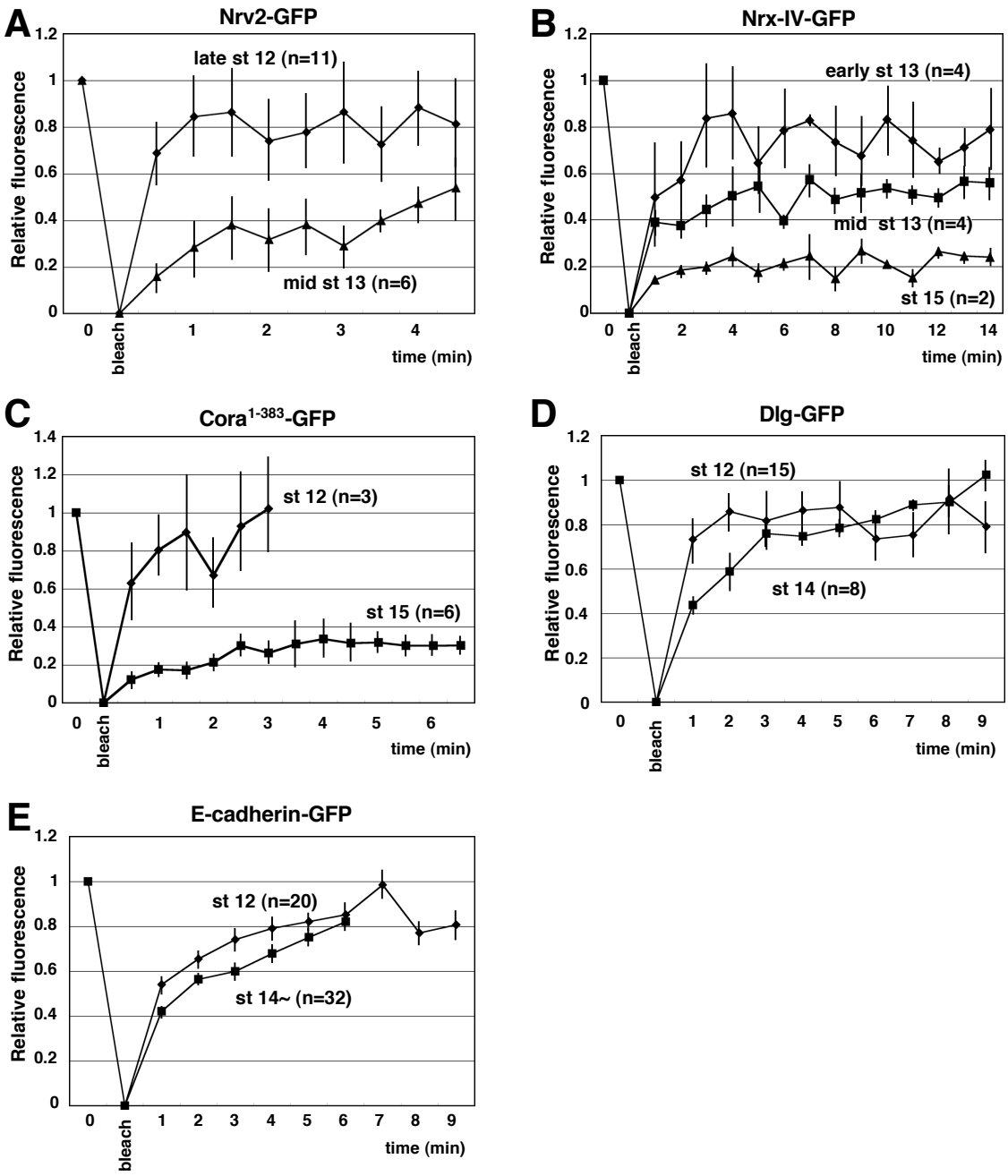
A
Nrv2-GFP
late st 12 (n=11)
mid st 13 (n=6)
Relative fluorescence
bleach
time (min)
B
Nrx-IV-GFP
early st 13 (n=4)
mid st 13 (n=4)
st 15 (n=2)
Relative fluorescence
bleach
time (min)
C
Cora1-383-GFP
st 12 (n=3)
st 15 (n=6)
Relative fluorescence
bleach
time (min)
D
Dlg-GFP
st 12 (n=15)
st 14 (n=8)
Relative fluorescence
bleach
time (min)
E
E-cadherin-GFP
st 12 (n=20)
st 14~ (n=32)
Relative fluorescence
bleach
time (min)

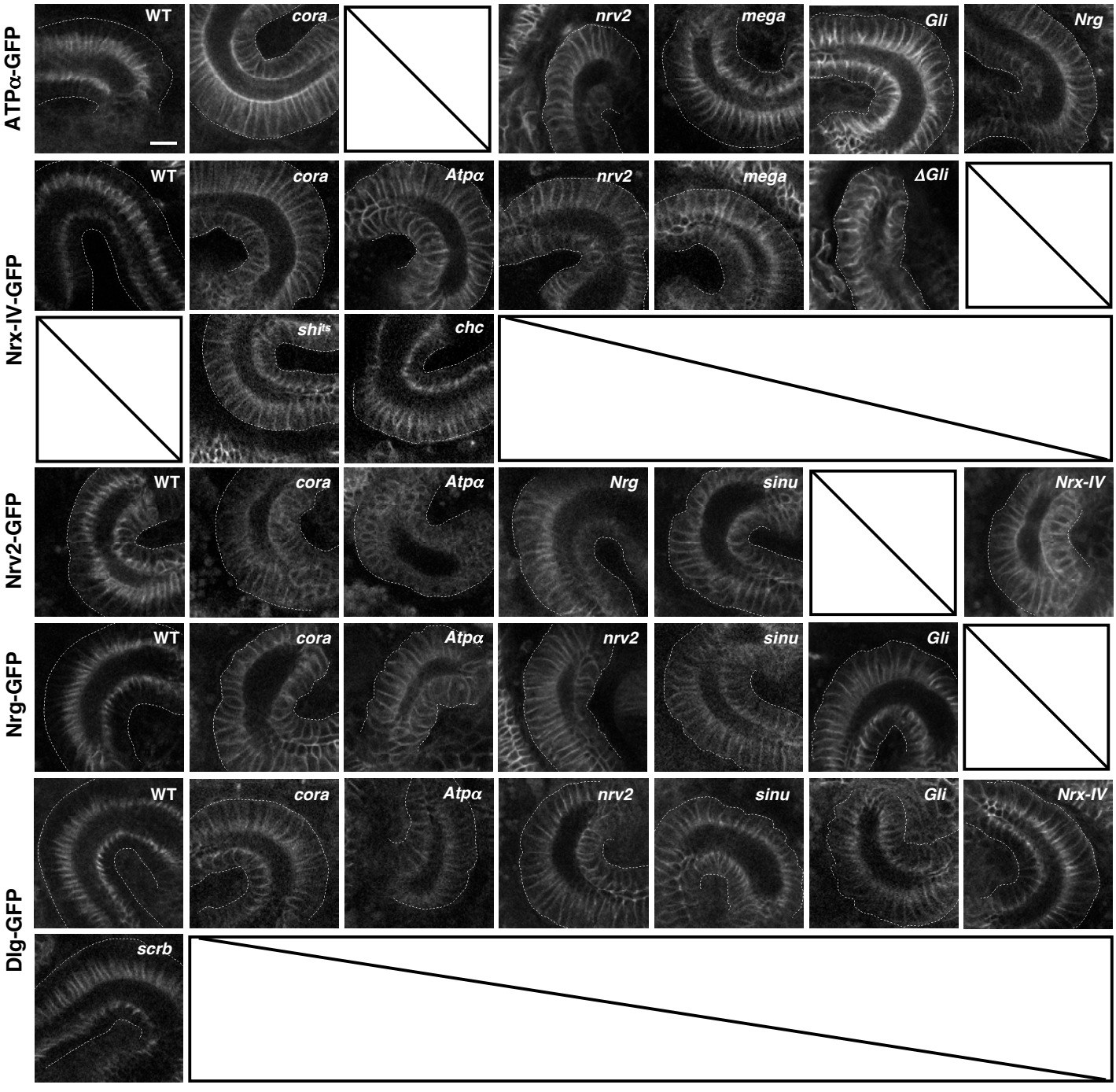
ATPα-GFP
WT
cora
nrv2
mega
Gli
Nrg
Nrx-IV-GFP
WT
cora
Atpα
nrv2
mega
ΔGli
shi^ts
chc
Nrv2-GFP
WT
cora
Atpα
Nrg
sinu
Nrx-IV
Nrg-GFP
WT
cora
Atpα
nrv2
sinu
Gli
Dlg-GFP
WT
cora
Atpα
nrv2
sinu
Gli
Nrx-IV
scrb

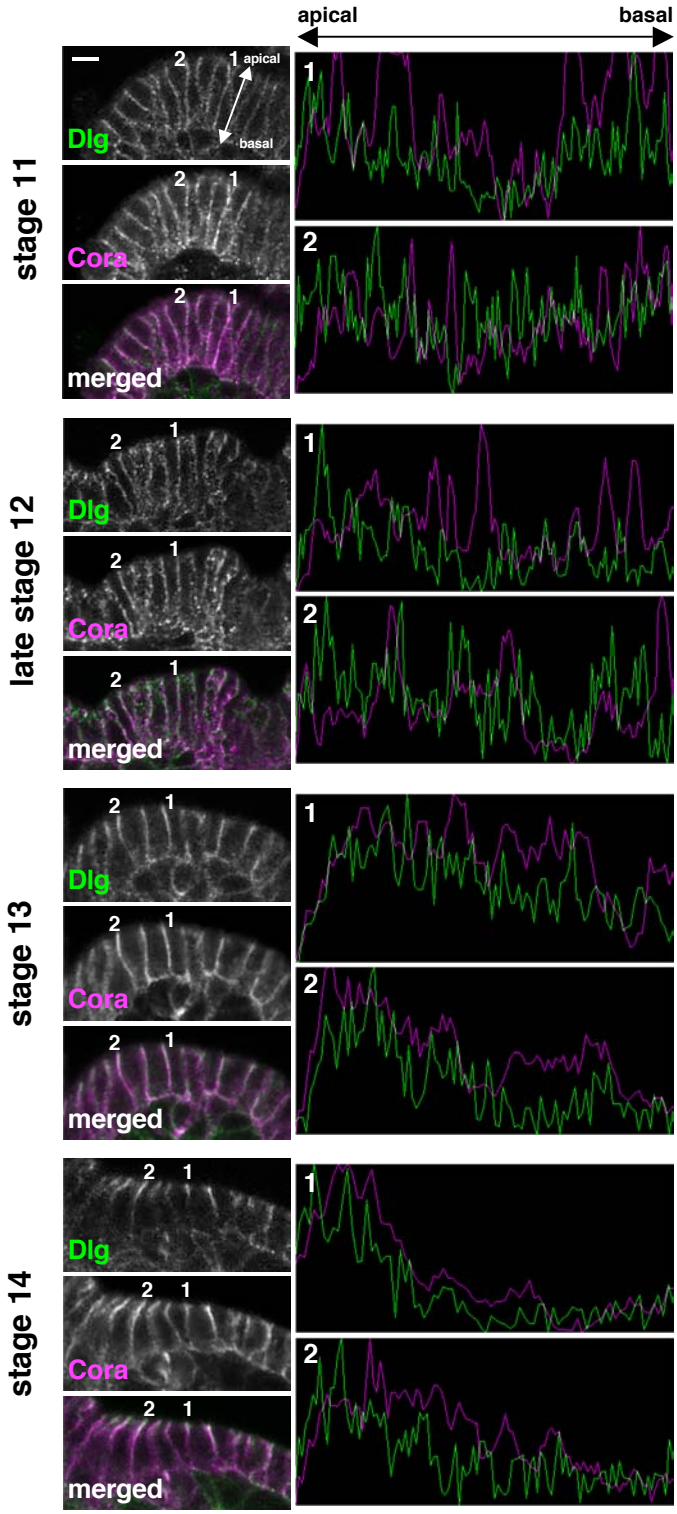
apical
basal
stage 11
late stage 12
stage 13
stage 14
Dlg
Cora
merged
apical
basal
1
2

Table S1. Genotypes used to examine GFP-tagged proteins in SJ mutant backgrounds

1. *Nrg^{14}/FM7a, dfd-GMR-YFP; Atpα-GFP/+*
2. *mega^{G0012}/FM7a, dfd-GMR-YFP; Atpα-GFP/+*
3. *cora^{5}/CyO, dfd-GMR-YFP; Atpα-GFP/+*
4. *nrv2^{23B}/CyO, dfd-GMR-YFP; Atpα-GFP/+*
5. *Df(2L)Exel7079/CyO, dfd-GMR-YFP; Atpα-GFP/+*
6. *Gli^{1}/CyO, dfd-GMR-YFP; Atpα-GFP/+*
7. *Nrg^{14}/FM7a, dfd-GMR-YFP; nrv2-GFP/+*
8. *mega^{G0012}/FM7a, dfd-GMR-YFP; nrv2-GFP/+*
9. *bou^{GG01077}/FM7a, dfd-GMR-YFP; nrv2-GFP/+*
10. *nrv2-GFP cora^{5}/CyO*
11. *nrv2-GFP/+; Atpα^{01453a} /TM6B, dfd-GMR-YFP Sb^{1} Tb^{1}*
12. *nrv2-GFP/+; Nrx-IV^{14}/TM6B, dfd-GMR-YFP Sb^{1} Tb^{1}*
13. *nrv2-GFP/+; sinu^{nwu7}/TM6B, dfd-GMR-YFP Sb^{1} Tb^{1}*
14. *Nrg^{14}/FM7a, dfd-GMR-YFP;; Nrx-IV-GFP/+*
15. *Chc^{1}/FM7a, dfd-GMR-YFP;; Nrx-IV-GFP/+*
16. *shi^{ts}/FM7a, dfd-GMR-YFP;; Nrx-IV-GFP/+*
17. *mega^{G0012}/FM7a dfd-GMR-YFP; Nrx-IV-GFP/+*
18. *bou^{GG01077}/FM7a, dfd-GMR-YFP; Nrx-IV-GFP/+*
19. *cora^{5}/CyO, dfd-GMR-YFP; Nrx-IV-GFP/+*
20. *nrv2^{23B} /CyO, dfd-GMR-YFP; Nrx-IV-GFP/+*
21. *Gli^{1}/CyO, dfd-GMR-YFP; Nrx-IV-GFP/+*
22. *Df(2L)BSC255/CyO, dfd-GMR-YFP; Nrx-IV-GFP/+*
23. *crok^{KG06053}/CyO, dfd-GMR-YFP; Nrx-IV-GFP/+*
24. *cold^{f02238}/CyO, dfd-GMR-YFP; Nrx-IV-GFP/+*
25. *Nrx-IV-GFP Atpα^{01453a}/TM6B, dfd-GMR-YFP Sb^{1} Tb^{1}*
26. *Nrg-GFP/+; cora^{5}/CyO, dfd-GMR-YFP*
27. *Nrg-GFP/+; nrv2^{23B}/CyO, dfd-GMR-YFP*
28. *Nrg-GFP/+; Gli^{1}/CyO, dfd-GMR-YFP*
29. *Nrg-GFP/+; sinu^{nwu7}/TM6B, dfd-GMR-YFP Sb^{1} Tb^{1}*
30. *Nrg-GFP/+; Atpα^{01453a}/TM6B, dfd-GMR-YFP Sb^{1} Tb^{1}*
31. *Nrg-GFP/+; Df(3R)ED10811/TM6B, dfd-GMR-YFP Sb^{1} Tb^{1}*
32. *Nrg-GFP/+; Df(3L)ED4470/TM6B, dfd-GMR-YFP Sb^{1} Tb^{1}*
33. *Dlg-GFP/+; cora^{5}/CyO, dfd-GMR-YFP*
34. *Dlg-GFP/+; nrv2^{23B}/CyO, dfd-GMR-YFP*
35. *Dlg-GFP/+; Gli^{1}/CyO, dfd-GMR-YFP*
36. *Dlg-GFP/+; Atpα^{01453a}/TM6B, dfd-GMR-YFP Sb^{1} Tb^{1}*
37. *Dlg-GFP/+; Nrx-IV^{14}/TM6B, dfd-GMR-YFP Sb^{1} Tb^{1}*
38. *Dlg-GFP/+; sinu^{nwu7}/TM6B, dfd-GMR-YFP Sb^{1} Tb^{1}*
39. *Dlg-GFP/+; scrib^{2}/TM6B, dfd-GMR-YFP Sb^{1} Tb^{1}*
40. *cora^{5} Ubiquitin-gal4/CyO, Kr-GFP*
41. *cora^{5} UAS-E-cadherin-GFP/CyO*